Hydration mechanism in Ce-exchanged zeolites and heat release performances upon adsorption of water vapour in support of their potential use in thermochemical storage of energy under mild conditions of adsorbent regeneration and saturation

Hao Wu, Philippe Trens, Bernard Fraisse, Fabrice Salles, Jerzy Zajac

Hydration mechanism in Ce-exchanged zeolites and heat release performances upon adsorption of water vapour in support of their potential use in thermochemical storage of energy under mild conditions of adsorbent regeneration and saturation

Hao Wu, Philippe Trens, Bernard Fraisse, Fabrice Salles*, Jerzy Zajac*

Institut Charles Gerhardt (ICGM), Université de Montpellier, CNRS, ENSCM. Place Eugène Bataillon, 34095 Montpellier Cedex 5, France,

E-mail: fabrice.salles@umontpellier.fr, jerzy.zajac@umontpellier.fr

Keywords: 13X zeolite, cation exchange, trivalent and tetravalent cerium, water vapour adsorption, cation distribution, adsorption isotherms, heats of adsorption, gas flow calorimetry, Monte Carlo simulations, thermochemical energy storage, mild adsorbent regeneration and saturation

Abstract

The potential use of commercially available 13X zeolite, modified by ion-exchange with cerium compensating cations possessing high charges and high hydration energies, has been tested in view of low-temperature storage of solar energy performed under mild operating conditions of low regeneration temperatures and low pressures of water vapour during the adsorption step. Structural and textural properties, sorption behaviour towards water vapour of three selected samples containing various proportions of Ce^{3+} and Ce^{4+} compensating cations and the pristine Na^{+}-13X zeolite were studied by a variety of experimental techniques including Wavelength Dispersive X-Ray Fluorescence, Energy Dispersive X-ray Spectroscopy, X-ray diffraction, Thermogravimetric analysis, as well as measurements of the adsorption of gaseous nitrogen at 77 K and water vapour at 313 K. Based on the structure refinement procedure applied to the experimental XRD patterns, it was demonstrated that extra-framework cerium cations were preferentially located on sites I' and II in dry and hydrated zeolites, showing relatively little dependence on the hydration level. Monte Carlo simulations were used to determine the limit values of the amount adsorbed and differential heat of adsorption, which could be obtained

experimentally if the zeolite samples were completely dried. The potential of Ce-containing zeolites as adsorbents for the thermochemical energy storage was finally determined under flow conditions by firstly dehydrating samples at 353 K or 423 K and then saturating them at 296 K with water vapour at a mole fraction of 0.03. The choice of the operating conditions was decided so as to maintain the stability of the zeolite structure while taking the risk of reduced thermal performance of zeolite adsorbents undergoing incomplete regeneration-dehydration. Under such mild conditions, the modified 13X zeolites exhibited enhanced thermal performance in comparison with that of the pristine 13X, by releasing between 700 and 1100 kJ per kg of the adsorbent during a period of 6-8 hours. By a complementary study between calorimetry measurements and molecular simulations, the elucidation of the hydration-dehydration of Ce-exchanged zeolites coupled with cation displacements upon hydration has allowed to determine the best compromise for the regeneration of zeolites in the case of heat reallocation applications

Introduction

The rapidly increasing demand for energy, combined with the decrease of fossil fuel resources and growing greenhouse emissions, calls for the continued development of ambitious alternatives to move towards a sustainable, renewable and environment-friendly way to provide energy. Nowadays, renewable energy sources are considered as a key issue for sustainable development and climate change, especially in the building sector which is responsible for approximately 40% of the energy consumed in the EU countries resulting in strong greenhouse gases emissions [1]. In attempts to circumvent issues due to the intermittent nature of the renewable energy, many studies have focused on converting it into more useful forms such as thermal energy or electricity [2–6]. Amongst the numerous possibilities for energy conversion, solar energy harvested in abundance during summer may be exploited to increase the internal energy of an appropriate storage material (i.e., *charging step*) and thus be stored until cold days in winter when the heating supply system is under pressure. Converted subsequently into heat during the *discharging step*, it may be used as a supplemental source of space heating [6].

In view of future uses in low-temperature thermochemical storage of solar energy, solid materials capable of releasing much heat during adsorption of vapours have the potential to yield high storage densities [5,6]. With the open sorption systems operating in the moist-air flow mode, the heat released upon the adsorption of water vapour may serve to increase the temperature of the dry air leaving the reactor. The warm gas is subsequently directed to the

space heating loop of the heated building. Various kinds of solid materials with a propensity for being reversibly dried and hydrated, and additionally characterised by good hydrothermal stability, have been already tested as adsorbents for the thermochemical storage (TCS) uses [6–15]. Porous zeolites and zeolite-based structures commonly stand out from the others as combining high specific surface areas, pronounced hydrophilic character of their surface, and good thermal/hydrothermal stability [16,17]. By the way, zeolite 13X was the first adsorbent practically applied in a short-term low-temperature thermochemical storage for daily heating of a school building in Germany [18,19]. Nevertheless, the handling of zeolites as effective adsorbents of water vapour may pose some practical problems [6].

Firstly, when the zeolite-water affinity is strong even at low humidity levels, the adsorption isotherm is similar to the Type I curve possessing a very steep initial portion. In order to ensure the complete regeneration of the adsorbent after each discharging-hydration stage, harsh drying conditions are necessary (e.g., deep vacuum treatment at high temperatures). Furthermore, the use of an almost perfectly tight tank is imposed on the storage of the dried adsorbent between the successive charging and discharging steps so as to avoid the presence of water traces inside it. Otherwise, the adsorbent will be deactivated in an uncontrolled manner before the next discharging. Secondly, 13X-type zeolites subject to a great number of repeated drying-hydration cycles even at somewhat lower temperatures appear to undergo a progressive amorphisation and the concomitant evolution of the pore structure [20].

One possible solution to this issue could be to modulate the hydrophilic character of zeolite surface either by cation exchange or to modify the substitution ratio [21]. For example, it was proven that the nature of extra-framework cations had a strong influence on the hydration energy in porous solids [22–26]. Going further in this direction, commercially available 13X samples, containing mostly Na^+ as extra-framework compensating cations and subsequently modified by a partial ion exchange with divalent Ca and Mg cations, were demonstrated to yield interestingly enough amounts of heat during the adsorption of water vapour if the activation procedure had been performed at 473 K [26]. However, the migration of extra-framework cations among various crystallographic sites, which accompanies hydration and dehydration sequences [27,28], may be undesirable for long-term control of the TCS system.

The main objective of the present work was to design a cation-exchanged 13X zeolite with enhanced heat release characteristics, thus allowing avoiding the regeneration cycle to be performed under harsh conditions. Therefore, the main challenge was to increase the heat evolved upon the adsorption of water vapour onto a zeolite structure that had not been completely dehydrated in the preceding desorption step. The migration of compensating cations

upon hydration-drying stages to be reduced as much as possible was also targeted in the present work. By referring to the research strategy developed previously [26], similar commercially available 13X sample was modified by substituting the pristine extra-framework ions with various cerium cations. The choice of cerium was dictated by the fact that this rare earth metal could form both Ce^{3+} and Ce^{4+} cations possessing high energies of hydration in aqueous solutions [29,30]. Therefore, the expected increase in the heat release when adsorbing water vapour at low humidity contents was predicted on this basis. Despite a decrease in the number of multivalent cations necessary to compensate the negative charge of the zeolite framework, the net energy gain was justified by a non-linear increase in the molar enthalpy of hydration when compared with the initial Na^+ counter-ion; e.g., -6325 kJ mol^{-1}, Ce^{4+}; -3365 kJ mol^{-1}, Ce^{3+}; -415 kJ mol^{-1}, Na^+, according to reference [29]. Furthermore, the capacity of cerium cations to adapt their electronic configuration to their local environment underlying their particular redox properties was also taken into account [31]. Multi-scale experimental and modelling studies, including adsorption and batch calorimetry measurements, X-ray diffraction, and Monte Carlo simulations, were performed to elucidate the hydration mechanism occurring in the Ce-exchanged zeolite samples, as well as to optimise the regeneration conditions. The motion of the extra-framework cations in the structure was monitored by coupling X-Ray diffraction patterns with structural resolution and Monte Carlo simulations. Moreover, the heat release performances of the selected samples, in terms of the integral heat of adsorption and the kinetics of the heat evolvement, were evaluated based on the results of calorimetry measurements carried out with the aid of a gas flow microcalorimeter operating in the saturation mode. In the light of these results, the use of cerium-exchanged zeolites as adsorbents for the low-temperature thermochemical storage of energy by sorption was discussed.

Experimental section

Materials

High purity (ACS reagent grade, assay ≥ 99.0 %) cerium(III) nitrate hexahydrate, $Ce(NO_3)_3.6H_2O$, and ammonium sulfate, $(NH_4)_2SO_4$, were purchased from Sigma-Aldrich and employed without further purification. The 13X zeolite powder with a primary particle size of around 2 μm used in the present study was also a Sigma-Aldrich product. According to the technical specification, it contained only Na^+ as a compensating cation. The 18.2 MΩ cm

ultrapure water (PURELAB® Chorus 1, ELGA Veolia) was used in the synthesis and ion exchange procedures, as well as in the adsorption and calorimetry measurements. The gas adsorption and calorimetry experiments were carried out by making use of ALPHAGAZ 2 grade helium and nitrogen (Air Liquide, France).

Preparation of ion-exchanged zeolites

Three ion-exchanged 13X zeolite samples were prepared in the following way.

A stock 0.05 mol L^{-1} aqueous solution of Ce^{3+} was prepared by dissolving the $Ce(NO_3)_3.6H_2O$ powder in ultrapure water. After the addition of 1 g of 13X zeolite to 50 mL of this solution, the suspension was firstly stirred at 338 K for 3 hours and then centrifuged for 10 minutes at 11000 rpm. The solid sample was subsequently separated from the supernatant liquid. This procedure was repeated twice more, with the suspension stirring step being extended to 24 hours upon the last cycle. Then, the resulting solid sample was shaken again with 50 mL of ultrapure water at room temperature for two hours and centrifuged in the same way as before. The whole procedure was repeated 5 times, with the final stirring being prolonged to 24 hours. The solid was finally dehydrated by freeze-drying (lyophilisation) under vacuum in a Cryonext freeze-drier and stored in unsealed vials. The sample achieved in this way was denoted as Ce1-13X.

In order to maximise the exchange ratio, the pristine 13X sample was first washed with ultrapure water and a preliminary exchange step was then performed for 2 hours by using 50 mL of aqueous $(NH_4)_2SO_4$ solution. The aim here was to exchange the primary Na^+ cations for NH_4^+ ones and thus facilitate further exchange with cerium. Similar exchange procedure was carried out twice making use of 50 mL of solution containing Ce^{3+} at a concentration of 0.005 mol L^{-1}. The purification and drying procedures were the same as before. The resulting sample was named as Ce2-13X.

An additional zeolite sample containing a great quantity of Ce^{4+} as a compensating cation was also prepared. According to Hunter [32], oxidation of extra-framework Ce^{3+} to Ce^{4+} was possible upon calcination of the zeolite structure at high temperatures in air. For this purpose, a part of the Ce2-13X sample was heated at 723 K in air during 12 hours. As a result, a change of colour was observed from white to pale yellow thus indicating the oxidation of Ce(III) to Ce(IV). This sample was referred to as Ce3-13X.

Zeolite sample characterization

The chemical formulas of the initial 13X and Ce^{3+}-exchanged 13X samples were determined with the aid of Wavelength Dispersive X-Ray Fluorescence (WDXRF) spectrometer (Axios Max, PANalytical) and Energy Dispersive X-ray Spectroscopy (EDX) on the scanning electron microscope (SEM) (FEI Quanta 200 FEG). Since it was not possible to find the proportion between Ce^{3+} and Ce^{4+} in Ce3-13X, the chemical formula of this sample remained undetermined.

Textural properties of the solids were characterized based on the gaseous nitrogen adsorption isotherms measured at 77 K using a micromeritics ASAP2010 sorption equipment. Samples were degassed at 473 K for 12 h under secondary vacuum prior to adsorption measurements. The apparent specific surface areas were then calculated on the basis of the BET model by taking 0.162 nm^2 as a cross sectional area for one adsorbed N_2 molecule [33].

Some characteristics of the pristine 13X zeolite and cerium-exchanged samples tested in the present study are given in Table 1.

Table 1. Chemical formula, atomic Si:Al ratio, degree of cation exchange, and apparent specific surface area for the zeolite samples studied.

Sample	Chemical formula	Si:Al	Exchange ratio (%)	S_{ap} ($m^2\ g^{-1}$)
13X	$Na_{87,8}(SiO_2)_{108,9}(AlO_2)_{83,1}$, xH_2O	1.27	-	519
Ce1-13X	$Na_{10,6}Ce_{24,2}(SiO_2)_{109,6}(AlO2)_{82,4}$, xH_2O	1.33	88	426
Ce2-13X	$Na_{2,6}Ce_{27,4}(SiO_2)_{109}(AlO_2)_{83}$, xH_2O	1.31	97	661

N.B. An apparent specific surface area of 578 $m^2\ g^{-1}$ was determined for Ce3-13X

Thermogravimetric analysis (TGA) was performed on a NETZSCH Jupiter STA 449, under an argon flow of 50 mL min^{-1}. Samples were heated from 298 K to 823 K in an alumina crucible by using a heating ramp of 5°C min^{-1}.

The resistance of the zeolite structure to cation exchange was monitored by X-ray diffraction (XRD) at room temperature when exposing powder samples to Cu-K_α X-ray radiation with the aid of Philips X'Pert PRO MPD equipped with an X'Celerator Scientific detector using 0.04 rad Soller slits. The same radiation source was used in the *in situ* XRD

analysis at high temperatures on a Panalytical Empyrean diffractometer with Pixcel3D detector, using 0.02 rad Soller slits to prevent axial divergence and thus improve peak shape and symmetry. This XRD equipment included an Anton Paar HTK16 chamber with platinum heating filament, which offered the possibility of working in static air atmosphere at various temperatures. The zeolite particles were suspended in a few drops of water and deposited on a 10% rhodium-platinum slide to form a thin and uniform layer at the end of water evaporation process. The subsequent desorption of water from the surface was achieved by starting with a completely hydrated sample at room temperature, firstly, and then by increasing the temperature step by step. This facility was used to obtain the XRD patterns for Ce^{3+}-containing samples successively at 303, 353, 423, 573, and 723 K, thus simulating different hydration states. The diffraction data were quantitatively analysed using the Rietveld refinement approach mostly with the aim of determining the extra-framework positions of charge-compensating cations. The recorded XRD patterns were refined by using Le Bail method and the SUPERFLIP software to solve the crystal structure of Ce-exchanged zeolites at different hydration states [34]. Furthermore, the JANA2006 software was employed to refine the crystal structure [35] and specify the location of cerium cations.

Measurements of the adsorption of water vapour in various experimental regimes

The adsorption of water vapour under static equilibrium conditions was studied at 313 K by means of a home-made apparatus previously described in the literature [36]. Prior to the adsorption measurements, the zeolite samples underwent an initial thermal treatment at 423 K under a vacuum pressure of 10^{-5} Torr. For the purpose of the experiment, the temperature of the thermoregulated chamber was set to 313 K and an adsorption curve was determined based on the manometric/volumetric measuring principles. More precisely, the vapour pressure is measured before and after the sorption step. Assuming the vapour as a perfect gas, the difference in pressure induced by sorption could be related to the adsorbed amount, after a careful determination of the sample cell volume. One particular interest of our sorption device is the possibility to set the initial pressures rather than the equilibrium pressure. This possibility allows the sample itself to define the number of data in the sorption isotherm. Indeed, in the next sorption step, the initial pressure will be calculated by adding the equilibrium pressure measured in the former step to a defined vapour pressure. REF ("Adsorption and separation of xylene isomers vapors onto the chromium terephthalate-based porous material MIL-101(Cr): An experimental and computational study", Trens, Philippe, Belarbi, Hichem, Shepherd, Celine, Gonzalez, Philippe, Ramsahye, Naseem A, Lee, U-Hwang, Seo, You-Kyong, Chang, Jong-

San, MICROPOROUS AND MESOPOROUS MATERIALS, Volume: 183, Pages: 17-22, 2014).

The uncertainties of the measurements can be evaluated by the slight scattering of the data in the sorption traces. However, the adsorbed amounts at saturation (see later) are consistent with former results published on similar materials. (WATER SORPTION AND DESORPTION ISOTHERMS OF SOME NATURALLY-OCCURRING ZEOLITES, YAMANAKA, S; MALLA, PB; KOMARNENI, S, ZEOLITES, Volume: 9, Issue: 1, Pages: 18-22, 1989).

The use of a Calvet-type differential and isothermal microcalorimeter (Setaram instrumentation C80) connected to the static volumetric rig allowed the differential molar heat of adsorption to be additionally measured [37].

The heat release performances of the zeolite samples were also evaluated under dynamic conditions by applying a 4 V ms Microscal flow microcalorimeter operating in a saturation mode [38]. Helium was used as a carrier gas at a flow rate of 2 mL min^{-1}. Each adsorbent was pre-activated in a flow of argon at 423 K during 24 h in a separate degassing rig outside the calorimeter. A weighted solid sample (about 80 mg) was introduced to fill a 50 µL calorimetric cell. The sample was subsequently flushed with helium to reach the initial thermal equilibrium. An in-line mounted saturation vessel filled with ultrapure water and thermostated by a water bath was used to continuously saturate the flowing helium with water vapour at 296 K. After having attained a steady thermal baseline, the flow of helium containing water vapour at a partial pressure of 2.8 kPa was directed to the calorimetric cell still at a constant flow rate of 2 mL min^{-1}. The complete saturation of the zeolite sample with water vapour was decided on the basis of the return of the thermal signal to baseline. Calibration of the areas under the thermal profile was carried out by dissipating a known amount of energy in the cell, with the aid of a calibration probe placed directly within the adsorbent bed, under the same flowing conditions and integrating the related exothermic peaks. The total amount of heat released during each saturation run corresponded to the integral heat of adsorption. After the saturation stage, the adsorbent was degassed under a constant flow of helium. This regeneration step lasted 1 day and night, with the adsorbent being heated at 353 K during 24 h and then cooled down to room temperature overnight. Altogether, three degassing-saturation cycles were performed for each zeolite sample.

Computational section

Grand Canonical Monte Carlo (GCMC) simulations were performed using a home-made code to localize the position of extra-framework cations and evaluate the sorption

properties of the investigated zeolite structures. To reproduce the 13X zeolite structure, the space group *Fd*3*m* with a unit cell parameter of 24.85 ± 0.03 Å was considered [39]. In the unit cell, 16 hexagonal prisms, 8 sodalite cages, and 8 supercages composed the structure, thus resulting in a general chemical formula of $M_x/nAl_xSi_{192-x}O_{384}\cdot yH_2O$, with M^{n+} being a given compensating cation: *x* varied from 0 to 96, *y* corresponded to the number of water molecules in the unit cell. In the present study, the atomic Si/Al ratio ranged between 1.0 and 1.5 and a rigid framework was considered; i.e., 88 substitutions of Si^{4+} by Al^{3+} distributed randomly following the Loewenstein's rule.

In order to predict the adsorption enthalpies and isotherms, a standard methodology is used, based on the equilibrium of chemical potentials between the adsorbed phase in the pores and the gaseous phase at a given temperature. In our case, temperature, chemical potentials for water vapour and unit cell volume are kept as fixed. The interactions between adsorbate molecules and the solid are then calculated by 12-6 Lennard Jones and electrostatic potentials.

During the GCMC simulations, the 3D periodic boundary conditions are applied, while the moves for water molecules include translation, rotation, deletion and insertion randomly considered during the equilibration steps.

Computations were performed at 298 K using 10^7 Monte Carlo production steps following 10^7 equilibration steps. The partial atomic charges (see Table S1 in Supplementary Material) and the 12-6 Lennard-Jones (LJ) atomic parameters for the framework were taken from the literature [26] and the UFF respectively, while formal charges and UFF were used for the extra-framework cations. Water molecules were considered as rigid by using the four-site charged LJ TIP4P/2005 model [26].

The parameters of the adsorbate/adsorbent LJ interatomic potential were then calculated using the Lorentz-Berthelot combining rule. A cut-off radius of 12 Å was applied to all LJ interactions, and the long-range electrostatic interactions were handled by applying the summation Ewald technique. In these calculations, extra-framework cations were allowed to move within the porous structure.

Results and Discussion

Given the higher valence of cerium species and some changes of the textural parameters reported in Table 1, the question arises as to whether the zeolite structure has been preserved

after ion exchange with Ce^{3+} cations and also after oxidation from Ce^{3+} to Ce^{4+}. For this purpose, the three ion-exchanged zeolite samples and the pristine 13X material were studied by XRD. Figure 1 shows the experimental XRD patterns recorded for all samples at room temperature.

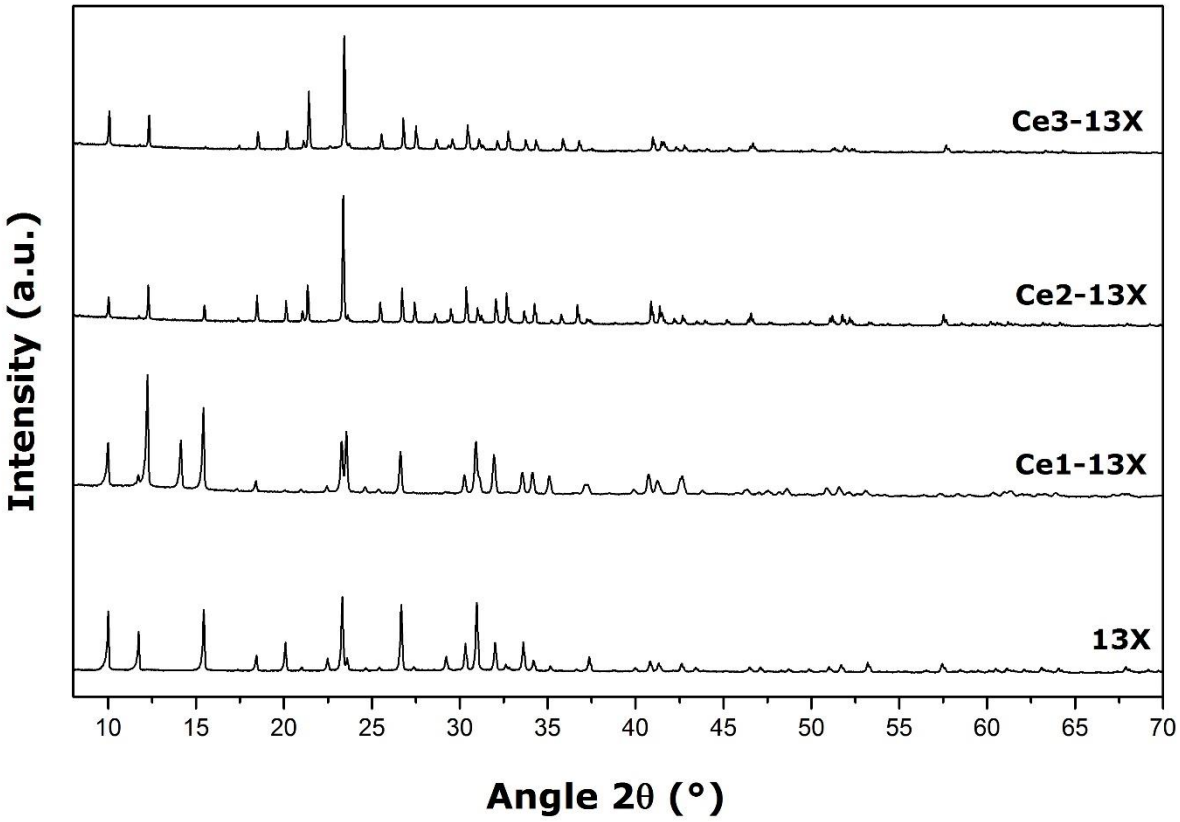

Figure 1. Room temperature X-ray diffraction patterns recorded for the pristine 13X, Ce1-13X, Ce2-13X, and Ce3-13X, as defined in the Experimental section.

Despite some changes in the relative intensity of the peaks observed in the XRD patterns in Fig. 1, the number and the positions of these peaks remain essentially the same. It can be thus concluded that ion exchange in the 13X faujasite does not induce great modification of the zeolite structure. This result supports the hypothesis that the structure is close to be rigid and behaves in this manner upon ion exchange, as has been already reported in the literature [40]. Furthermore, the number and valence of compensating cations have no impact on the structure since the peak positions in the XRD patterns of samples containing Ce^{3+} and Ce^{4+} are always the same. In all cases, the observed modification of the peak intensity can be ascribed to the modification of the electronic density inside the pores. Nevertheless, the XRD pattern of Ce1-13X presents an exception to the trends described above. Indeed, a new peak can be seen at a

2θ value of 13.2°. The comparison with the XRD pattern of the bulk $Ce(NO_3)_3.4H_2O$ (c.f., Figure S1 in Supplementary Material) provides a plausible argument that some quantity of non-reacted cerium salt has remained after ion exchange and purification procedures. Since a marked decrease in the apparent specific surface area has been inferred from the measurements of the gaseous N_2 adsorption isotherm for this sample, it seems reasonable to conclude that such cerium nitrate particles are irreversibly trapped within some pores of the zeolite. Certainly, the chemical formula and the ion exchange ratio reported in Table 1 are no longer valid. This sample with less defined characteristics is still of interest in view of the present application, especially when comparing with Ce2-13X characterised by an exchange ratio close to 100%.

Effects of temperature and hydration state

In the second stage, the effect of temperature and hydration state on the crystallographic positions of the atoms within the framework, as well as on the positions of the extra-framework cations was investigated. Several characteristic temperatures were selected in relation with the operating conditions under which zeolites 13X had been previously tested in the context of thermochemical storage of energy [3], as well as under which their dehydration or oxidation of Ce^{3+} to Ce^{4+} had been studied [32,41]. An example of *in situ* XRD patterns recorded at these different temperatures and hydration states is given in Fig. 2.

The X-ray diffractograms recorded on Ce1-13X have been chosen for illustrative purposes since this sample contains additional peaks compared to the others. For example, it is worth noting that the additional peak of bulk cerium nitrate is to a very great extent reduced after heating near and above 423 K, which supports well the previously forwarded hypothesis of its location outside the zeolite framework. Changes in the intensity of other diffraction peaks recorded at different temperatures indicate that the electronic density has been modified when raising the temperature. This modification of the electronic density can be attributed to changing positions of the extra-framework cations and progressive removal of the adsorbed water molecules. Indeed, an increase in the temperature induces the passage of the zeolite structure to a less hydrated state because of the enhanced evaporation of water. Such a decreasing loading in water inside the pores leads to observe a better crystallization and therefore to observe modifications for both the shapes and the intensity of the peaks (which also modifies the relative intensities for the complete diffractograms). This in turn may affect the mobility of the extra-framework cations [27,42]. It is important to note that the diffractograms recorded at 303 K in the beginning and at the end of the experiment are not strictly identical to each other. A net change in colour of the recovered sample additionally argues in favour of the irreversible

oxidation of extra-framework Ce^{3+} cations, which has occurred after complete dehydration of Ce1-13X and its heating likely at 723 K in the static air atmosphere inside the XRD chamber.

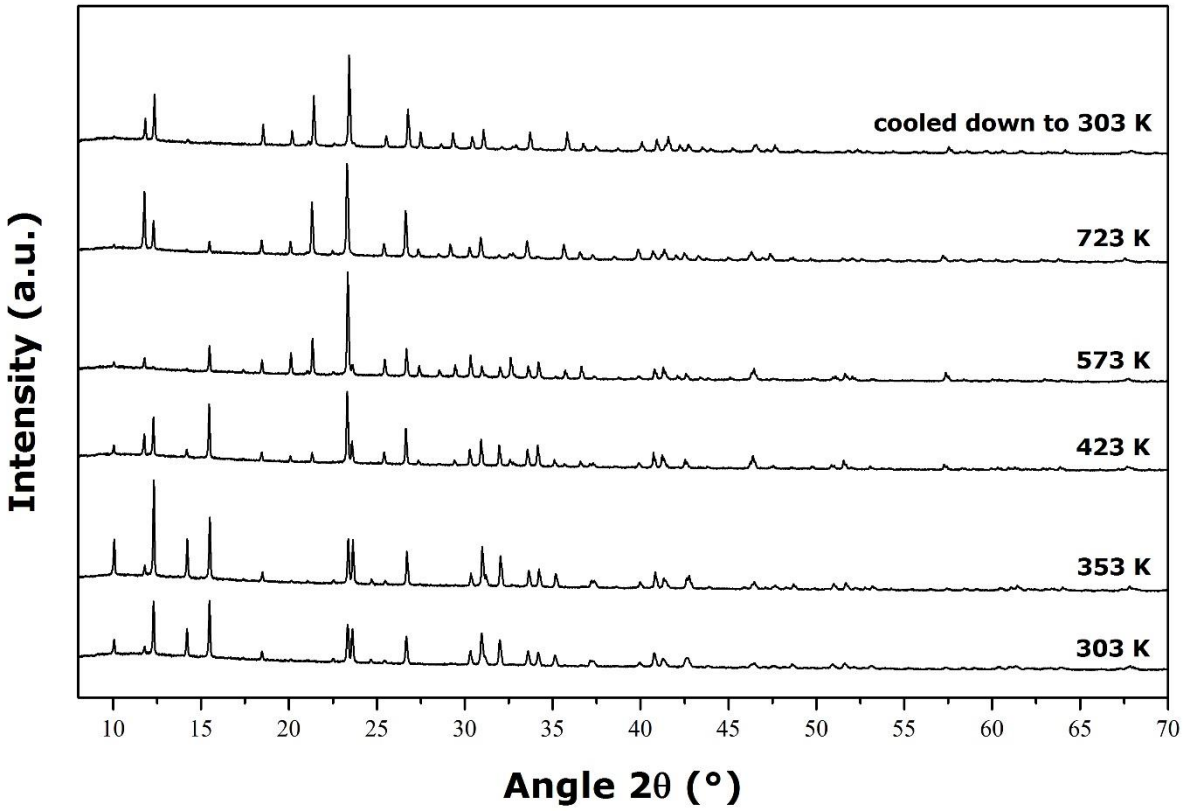

Figure 2. *In situ* XRD patterns recorded at different temperatures corresponding to a variety of hydration states for Ce1-13X. At the final state, the sample is cooled back to 303 K, after having been heated to 723 K.

Based on the XRD patterns recorded at various temperatures for zeolites exchanged with Ce^{3+}, the Rietveld method was used for the refinement of the zeolite structural model. In consequence, it was possible to analyse the location of extra-framework cations and to compare them with the theoretical positions inferred from Monte Carlo simulations. For computational purposes, two model zeolite structures saturated with Ce^{3+} and Ce^{4+} were considered, namely Ce^{3+}-13X and Ce^{4+}-13X. Some detailed results are reported in Supplementary Material: Figure S2 shows various crystallographic sites occupied by extra-framework cations in 13X zeolites; typical snapshots of the unit cell in the Ce-exchanged zeolites at different temperatures are given in Fig. S3 (structure refinement procedure), whereas those of the model Ce^{3+}-13X and Ce^{4+}-13X in dry and hydrated states are reproduced in Fig. S4 (Monte Carlo simulations).

For reasons of comparison between the experimental and theoretical results and in order to ensure the equivalence of various hydrated states, mass loss profiles of the zeolite samples studied as a function of the temperature, as obtained by means of thermogravimetric analysis (TGA), are given in Fig. S5 in Supplementary Material. The use of air has been avoided during the analysis period so as not to oxidize the compensating Ce^{3+} ions. The mass loss stops somewhat before 600 K in the case of 13X, whereas it still continues, although to a much lesser extent, above this temperature for Ce-containing samples. Much higher energies of cation hydration in aqueous solutions for Ce^{3+} and Ce^{4+} in comparison with that of Na^{+} can be taken into account to explain this trend, since higher temperatures will be necessary to remove last water molecules from the hydration shells surrounding the cerium compensating cations in the zeolite structures. Table 2 shows the percentage of mass loss measured until 3 temperatures envisaged for adsorbent regeneration.

Table 2. Percentage of mass loss monitored up to a given temperature for the zeolite samples studied. These values were calculated on the basis of thermogravimetric analysis (the corresponding TGA curves are reported in Fig. S5 in Supplementary Material).

Sample	13X	Ce1-13X	Ce2-13X	Ce3-13X
Temperature (K)	Mass loss (%)			
353	5	5	4	5
423	15	15	13	15
573	25	23	22	22

According to the results reported in Fig. S5 and in Table 2, nearly complete regeneration of adsorbents is possible only when the temperature is at least equal to 573 K. In consequence, the results of structure refinement at this temperature will be confronted with those obtained for the model Ce^{3+}-13X sample at the dry state. By analogy, the sample heated at 723 K will be regarded as simulating the dry state of 13X saturated with Ce^{4+} cations.

The positions of the extra-framework cations as inferred from structure refinement and Monte Carlo simulations are reported in Table 3.

Table 3. Positions of the extra-framework cations in the Ce-exchanged zeolite samples as inferred from structure refinement based on the experimental XRD patterns and Monte Carlo simulations. Various crystallographic sites occupied by extra-framework cations in 13X

zeolites are specified in Fig. S2 in Supplementary Material. The occupation rate on a given crystallographic site or within supercages (SC) is given by a number before the symbol of the site. Real adsorbents and models appearing on the same line are regarded as corresponding to similar hydration states.

Structure refinement			Monte Carlo simulation		
Temp. (K)	Dominant cation	Sites	Model	Hydration state	Sites
303	Ce^{3+}	4 I' + 22 II	Ce^{3+}-13X	hydrated	6 I' + 9 II + 9 III + 5 SC
353	Ce^{3+}	4 I' + 22 II			
423	Ce^{3+}	13 I' + 11 II			
573	Ce^{3+}	20 I' + 5 II	Ce^{3+}-13X	dry	7 (I + I') + 16 II + 6 III'
723	Ce^{4+}	31 I'	Ce^{4+}-13X	dry	8 (I + I') + 9 II + 5 III'
303	Ce^{4+}	31 I'	Ce^{4+}-13X	hydrated	6 I' + 3 II + 9 III' + 4 SC

Taking into account the results obtained from the structure refinement, the type I' and II sites represent the preferential positions for extra-framework cations in dry and hydrated zeolites. Furthermore, this method does not reveal much difference between the hydrated and dry states: a systematic shift from sites II towards sites I' is observed when the hydration degree decreases. When the sample is heated up to 353 K, the sample retains much water and the positions of Ce^{3+} cations do not change at all. Increasing further the temperature to 423 K already puts the sample in a state approaching the dry one. As a first important conclusion drawn from these observations, the hydration phenomenon has rather little effect on the location of extra-framework cations. This can be ascribed to the high charges of the Ce^{3+} and Ce^{4+} compensating cations, thus making their electrostatic interactions with the zeolite framework much stronger. The lack of pronounced hydration effect, being particularly pronounced in the case of 13X zeolite containing Ce^{4+} cations, is of high importance in the context of the use of these adsorbents in the thermochemical energy storage. These results are in fairly good agreement with the preferential crystallographic positions inferred from Monte Carlo simulations performed on 13X zeolite structures saturated with Ce^{3+} and Ce^{4+} compensating ions. Here the type I', II, and III sites have been identified as the main adsorption centres. It is worth noting that similar cation distributions have been already reported for zeolites containing Na^{+}, Cs^{+}, and Co^{2+} cations in the dry state [39,43–46]. Some cerium cations appear to be located close to the supercages in the hydrated samples. It may be argued that the high energy of supercage hydration is responsible for the migration of the extra-framework cations initially positioned

close to the supercages towards the positions localised inside these supercages. Note that Na^+ compensating cations were demonstrated to occupy crystallographic sites depending to a small extent on the hydration or dry state of the zeolite samples [44]. It should be also remembered that the repartition of the aluminium moieties within the framework can strongly influence the distribution of the extra-framework cations.

Sorption properties of the Ce-exchanged zeolite sample

Altogether, the molecular simulations have proven useful for elucidating the mechanism of water adsorption onto cerium-exchanged zeolites and the resulting redistribution of the compensating cations within the pores, in line with the earlier arguments advanced in the literature [47]. Once the pertinent structural properties of the Ce-exchanged zeolite samples had been determined, further studies were necessary to estimate the extent and energetics of adsorption onto these adsorbents.

The adsorption capacity towards water vapour obviously depends on the temperatures applied during the charging and discharging stages. For the purpose of the present study, the choice of these temperatures was dictated by the need to be close to the operating conditions frequently tested in a thermochemical storage with the use of 13X zeolites [3]. Therefore, the experimental adsorption isotherms were measured at 313 K after having submitted the samples to a vacuum treatment at 423 K. The quantity of water adsorption was plotted as a function of the relative vapour pressure (the saturation vapour pressure for water at 313 K is 7.4 kPa). In order to gain an idea about the maximum adsorption capacity, the theoretical adsorption curves were calculated for the model Na^+-13X, Ce^{3+}-13X and Ce^{4+}-13X samples by referring to Monte Carlo simulations performed at 298 K. The experimental and simulated adsorption isotherms have been collected in Figure 3.

The comparison between the experimental and simulated adsorption isotherms reveals two opposite trends with the type and proportion of the extra-framework compensating cation. Two portions of the adsorption curves particularly deserve to be analysed: the initial segment (almost linear) at very low relative pressures, which gives an idea about the affinity of the adsorbate for the adsorbent surface, and the one at higher relative pressures, providing an estimate of the total adsorption capacity of a given sample. On the experimental side, Ce2-13X (containing mostly Ce^{3+} as a compensating cation) and Ce3-13X (containing some proportion of Ce^{4+}) adsorb less water vapour than the pristine 13X sample (sodium form) at various relative pressures. Because the initial slopes are very similar, almost vertical, it is difficult to precisely deduce which material would generate stronger interactions with water molecules. This is

confirmed by the enthalpic curves shown in the inset of Figure 3. The extrapolations at zero coverage for both enthalpic curves are similar, at the limit of the uncertainties of these measurements.

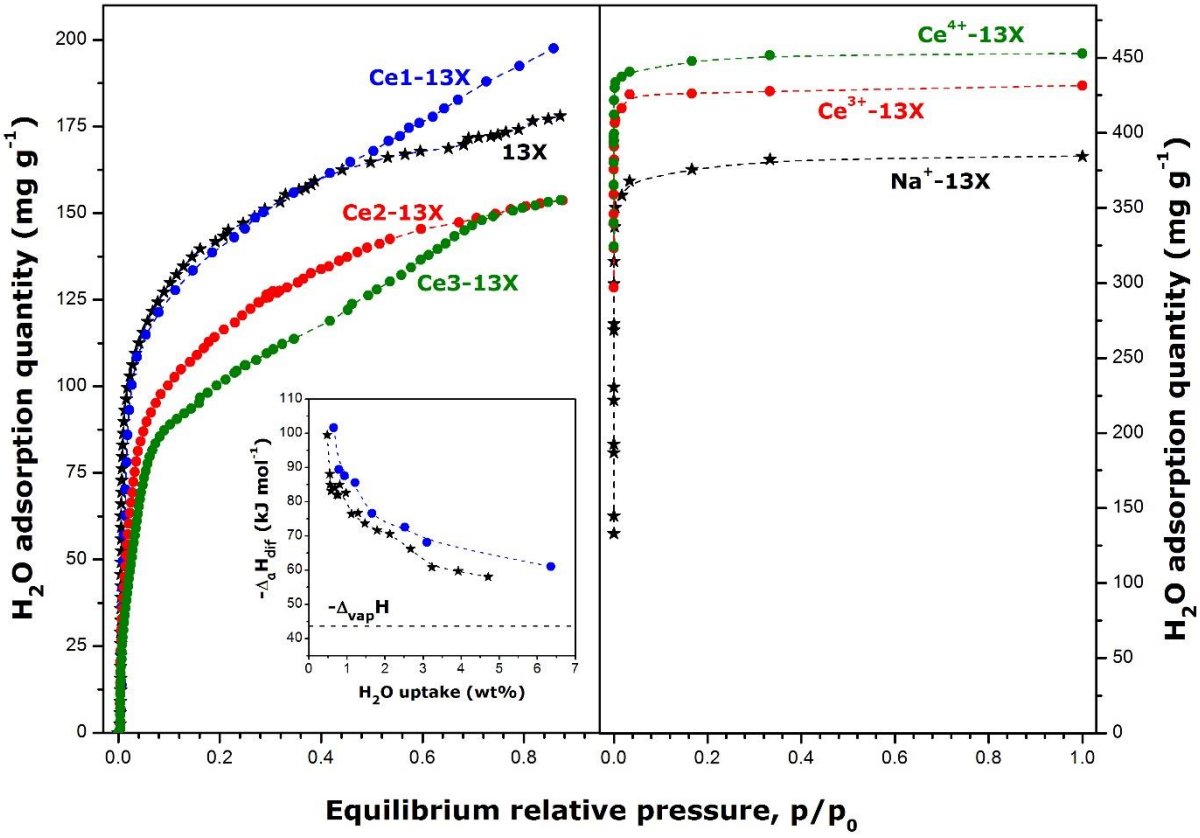

Figure 3. The experimental adsorption isotherms for water vapour onto various zeolite samples measured at 313 K after having submitted the samples to a relatively mild vacuum treatment at 423 K (left panel) and the theoretical adsorption curves for model zeolite samples obtained at 298 K by Monte Carlo simulations (right panel). The experimental and theoretical quantities of adsorption are presented here using two different scales. The inset within the left panel shows the variations of the differential molar heat of adsorption as a function of the water uptake for 13X and Ce1-13X in the initial adsorption range; the horizontal line represents the molar heat of water evaporation.

Furthermore, the two cerium-exchanged samples are characterised by similar adsorption capacities. Surprisingly, there is little difference in the quantity of adsorption between 13X and Ce1-13X, with the exception of the high pressure range where the latter adsorbs more water vapour. To better differentiate between these two samples with respect to their affinity towards

water, the variations of the differential molar heat of adsorption in the range of small quantities of water adsorption (up to about 7 wt%) are additionally illustrated in Fig.3. The differential heat, being of the order of 100 kJ per mole of water in the very beginning, decreases quickly with increasing adsorption values, in line with the energetic heterogeneity of the adsorption sites which are occupied by water molecules under the experimental conditions applied here.

On the basis of simulated adsorption isotherms, the adsorption capacity of the zeolite samples should move in the opposite direction: Na^{+}-13X < Ce^{3+}-13X < Ce^{4+}-13X. For very low relative pressures, the theoretical adsorption curves are superimposed on one another. The molar enthalpy of adsorption for the first water molecule was thus calculated with the aid of Monte Carlo simulations to gain an idea about the surface affinity towards water vapour. The following enthalpy values were obtained: -90 kJ mol^{-1}, Na^{+}-13X; -320 kJ mol^{-1}, Ce^{3+}-13X; -400 kJ mol^{-1}, Ce^{4+}-13X.

What is most important here is the acknowledgment that the quantities of water adsorption predicted by Monte Carlo simulations are much higher than those indicated by the adsorption experiments. To rationalise this finding, it is necessary to recall that the three model samples simulate the behaviour of the perfectly dried zeolite frameworks neutralised by one type of extra-framework cation. According to the results reported in the previous section, the temperature of thermal treatment applied (i.e., 423 K) is insufficient for complete adsorbent dehydration and some water molecules are likely present in the hydration shells which surround the compensating cations in the zeolite structures. In turn, the adsorption of such molecules would be more exothermic. Nonetheless, since they finally remain, in different quantities, in the samples treated at 423 K, the heat subsequently released during the adsorption of water vapour is markedly reduced compared to the theoretical heat amount that would have been obtained if the samples had been completely dehydrated. Another conclusion to be drawn from the comparison between the experimental and theoretical isotherms with respect to Ce3-13X may be that this sample rather contains a mixture of Ce^{4+} and Ce^{3+} compensating cations as a result of incomplete oxidation of Ce(III) to Ce(IV). There should be numerous Na^{+} cations still remaining in Ce1-13X after ion exchange, with much cerium being involved in the $Ce(NO_3)_3.4H_2O$ phase located within the pores. Finally, lowering the adsorption temperature from 313 K (experiment) to 298 K (simulations) increases the amount of water vapour retained by the zeolite sample in line with the exothermic character of the adsorption phenomenon.

Thermal performances of cerium-exchanged zeolites under flow conditions

The potential of Ce-exchanged zeolites as adsorbents for the thermochemical energy storage was finally considered by taking advantage of the results and conclusions presented in the previous sections. The operating conditions during the laboratory testing were defined mostly in line with the primary objective of the present study to reduce as much as possible the temperature of the adsorbent regeneration after a hydration stage performed at low pressures of water vapour. To minimize the mobility of the compensating cations, while avoiding the uncontrolled oxidation of Ce^{3+} ions, and thus to strengthen the stability of the zeolite structure submitted, in the industrial practice, to a large number of repeated regeneration-saturation cycles, it was decided to decrease the regeneration temperature down to 353 K (contrary to the temperature of 423 K applied previously in measurements under static conditions of equilibrium); the adsorption of water vapour was carried out at 296 K. Studies of the effect of the regeneration temperature on the extent and kinetics of water adsorption onto zeolite 13X from the gas phase reported in the literature were also the motivation underlying this change of the operating conditions. For example [41], it was shown that changes in the regeneration temperature between 353 and 393 K had no significant impact neither on the quantity of water adsorption nor on the effective diffusivity, the latter being rather decreased with an increase in the adsorbate concentration; the upward trend in the adsorption capacity was observed when decreasing the temperature of discharging (adsorption) and increasing the regeneration temperature from 393 to 423 K.

Gas flow calorimeter was used here as a measuring tool to determine the integral heat of adsorption when the solid sample placed in the calorimetric cell was saturated with water vapour at a partial pressure of 2.8 kPa (i.e., mole fraction of 0.03). Three dehydration-saturation cycles were performed for each zeolite sample under a constant flow of helium, either pure or containing water vapour, at a flow rate of 2 mL min^{-1}. Prior to the first saturation-degassing cycle, the adsorbent was activated by a vacuum treatment at 423 K. The resulting heat values are presented in the form of histogram bars in Fig. 4, whereas the corresponding heat release profiles are given in Fig. S6 in Supplementary Material.

It is clear from Fig. 4 that the cerium-exchanged samples are characterised by the enhanced heat release in comparison with the pristine 13X sample. The difference is particularly pronounced for the first saturation cycle. Here the saturation of Ce3-13X by water vapour under the experimental conditions applied yields more than 1100 kJ per kg of the sample, whereas integral heats of 950 and 800 kJ kg^{-1} are reported for Ce2-13X and 13X, respectively. When the vacuum treatment at 423 K is replaced by a flow of helium at 353 K, less energy is recovered upon the second and the third cycles: about 700 kJ kg^{-1} for the three cerium-exchanged zeolites

and 550-600 kJ kg^{-1} for 13X. This result emphasises again the importance of the regeneration temperature in the heat release cycle.

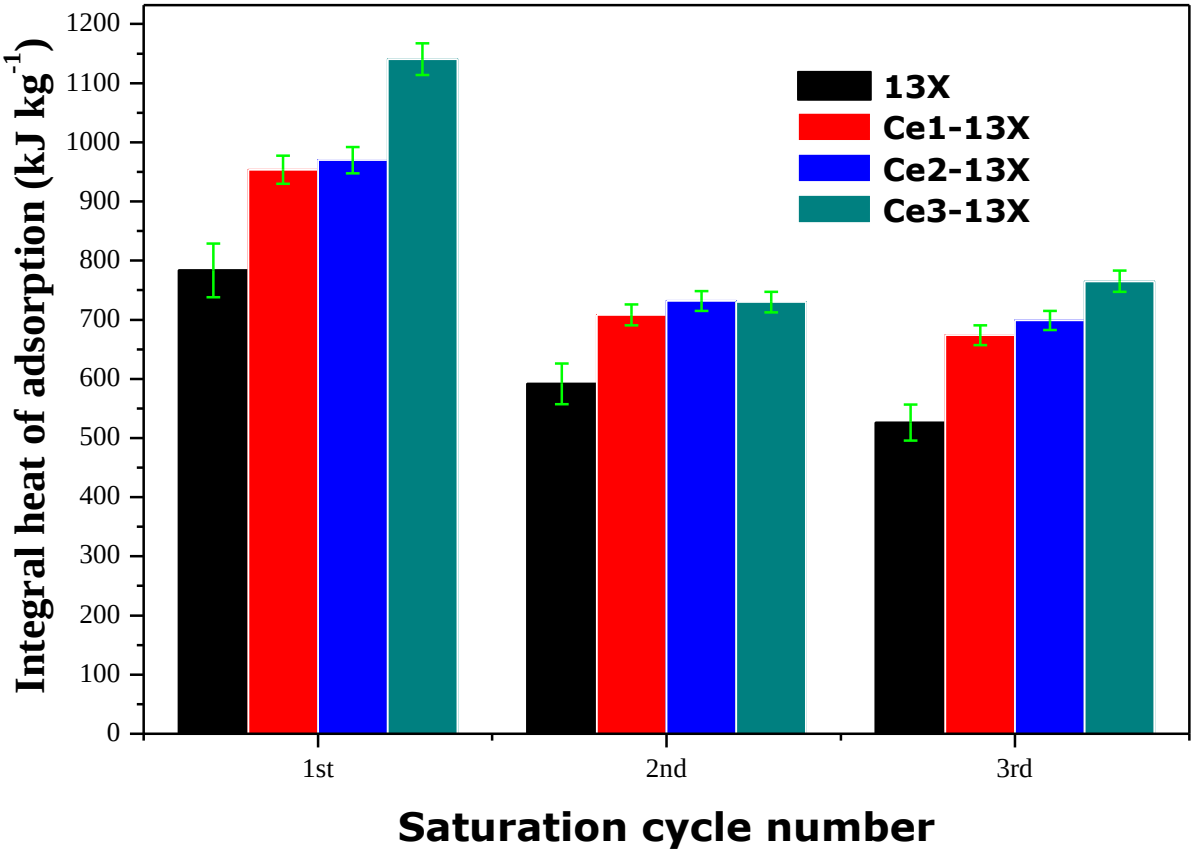

Figure 4. Integral heat of adsorption released during 3 consecutive saturation cycles for the zeolite samples studied after a regeneration stage performed by a flow of helium at 353 K. It is important to note that, prior to the first saturation-degassing cycle, the adsorbent was activated by a vacuum treatment at 423 K. Errors are reported with green symbols

In the case of cerium-exchanged samples, there is little difference between the integral heat values obtained in the second and third saturation stage, which means that the saturation-dehydration cycles become more regular at the end. For 13X, a marked decrease continues during the three cycles. In comparison with the thermal performance of the adsorbents achieved in the first adsorption stage after a more energy-consuming regeneration, between 64 and 74 % of the integral heat is still obtained in further dehydration-saturation cycles. This performance of Ce-exchanged zeolites is a good compromise when compared with the case of Mg- or Ca-exchanged zeolites for which, respectively, 810 and 310 kJ per kg of each sample were obtained during the first hydration after an initial vacuum pre-treatment at 473 K [26]. For the latter

zeolites, only 30-50% of the initial energy was recovered during next saturation cycles preceded by a regeneration at 298 K.

To underline again the importance of the regeneration and adsorption conditions, the limit values of the integral heat of adsorption were assessed on the basis of the theoretical chemical compositions for two model solids saturated with Ce^{3+} and Ce^{4+} compensating cations on one side, and the hydration energies of these cations in aqueous solutions, on the other side. The chemical formulas used in Monte Carlo simulations were as follows: $Ce_{29}NaSi_{104}Al_{88}O_{384}$ (molar mass = 15515 g mol^{-1}), Ce^{3+}-13X; $Ce_{22}Si_{104}Al_{88}O_{384}$ (molar mass = 14512 g mol^{-1}), Ce^{4+}-13X. By identifying the adsorption heat per one mole of compensating cation with its molar hydration heat and by dividing the final result by the molar mass of the model zeolite sample, it was possible to calculate the limit value of the integral heat of adsorption per kg of the solid. The following limit values were obtained: 6290 kJ kg^{-1}, Ce^{3+}-13X; 9590 kJ kg^{-1}, Ce^{4+}-13X. It is clear that the heat values determined for the Ce-containing samples in the present section are far from these limit values which could be reached experimentally if the completely dried samples were saturated with water vapour at saturated vapour pressure.

The kinetics of the heat evolvement also changes from one sample to another (c.f., Fig. S6 in Supplementary Material). At first sight, the heat release period lasts for 6-8 hours. In the case of pristine 13X sample, a gradual increase in the heat of adsorption is observed on either side of the central maximum attaining about 2 kJ kg^{-1} somewhere in the middle of the discharging period. A steeper increase in the heat release is observed in the beginning of the saturation cycle for Ce1-13X and the maximum is between 2.5 and 3.5 kJ kg^{-1}, depending on the cycle number. In consequence, this Ce-contained sample is characterised by a larger heat release window. As far as Ce2-13X and Ce3-13X are concerned, the plots of the instantaneous value of the heat released upon adsorption as a function of the discharging time represent left-skewed distribution curves; the maximum heat values are about 3.2 – 3.5 and 3.2 – 3.8 kJ kg^{-1}, respectively. Altogether, the Ce-exchanged samples provide relatively much heat over a rather short period of a few hours.

Conclusion

An alternative solution to harvest solar energy and store this energy as chemical potential without much energy loss can be proposed based on the adsorption of water vapour occurring in natural porous adsorbents, thus allowing the investment costs to be greatly reduced. Nevertheless, the main challenge is still to optimise the operating conditions corresponding to

the charging (adsorbent drying-regeneration) and discharging (vapour adsorption) stages, which may have negative effects on the hydrothermal stability of the adsorbent submitted to a large number of repeated regeneration-saturation cycles. Within the framework of the present study, the potential use of commercially available zeolites, modified by ion-exchange with cerium compensating cations possessing high charges and high hydration energies, was tested under mild operating conditions of low regeneration temperatures and low pressures of water vapour during the adsorption step.

A research approach combining experimental characterization techniques and theoretical methods was employed to monitor changes in the structural and textural properties of the zeolite samples as a function of the hydration state and oxidation number of extra-framework cerium cations. Based on the structure refinement procedure applied to the experimental XRD patterns, it was demonstrated that extra-framework cerium cations were preferentially located on sites I' and II in dry and hydrated zeolites, showing relatively little dependence on the hydration level. The experimental adsorption isotherms for water vapour onto cerium-containing zeolites and the pristine 13X sample were measured at 313 K after having submitted the samples to a vacuum treatment at 423 K. Monte Carlo simulations were used to determine the limit values of the amount adsorbed and differential heat of adsorption, which could be obtained experimentally if the zeolite samples were completely dried. The comparison between the experimental and theoretical values, together with the results of thermogravimetric analysis, provided strong evidence for the presence of water molecules in the hydration shells surrounding Na^{+}, Ce^{3+}, and Ce^{4+} compensating cations in the zeolite structures. The mobility of cerium cations in the Ce-exchanged zeolite structure was hindered when oscillating between room temperature and 353 K. The oxidation of Ce^{3+} ions to Ce^{4+} ones by heating at 723 K in air was found to be irreversible.

The potential of Ce-exchanged zeolites as adsorbents for the thermochemical energy storage was finally determined under flow conditions by firstly dehydrating samples at 353 K and then saturating them at 296 K with water vapour at a mole fraction of 0.03. The choice of the operating conditions was decided so as to maintain the stability of the zeolite structure while taking the risk of reduced thermal performance of zeolite adsorbents undergoing incomplete regeneration-dehydration. Three degassing-saturation cycles were carried out. Prior to the first saturation stage, the adsorbent was activated by a vacuum treatment at 423 K. Under such operating conditions, the cerium-containing samples were found to release between 700 and 1100 kJ per kg of the sample over a period of 6-8 hours, with the highest heat being reported for the zeolite sample containing Ce^{4+} compensating cations during the first saturation cycle.

Higher heat values compared to those attained for the pristine 13X zeolite under the same conditions argued in favour of the enhanced thermal performance of cerium-containing zeolites sufficiently enough to envisage the periodic heat release during the discharging step of the thermochemical storage performed under mild operating conditions.

Acknowledgement:

One of the authors, H. Wu, greatly acknowledges the financial support of his work by French Ministry of National Education, Higher Education and Research. The authors also want to thank J. Fullenwarth and Dr. N. Donzel of the Platform of Analysis and Characterisation (PAC), Pôle Chimie Balard, for their assistance, respectively, in X-ray Fluorescence and N_2 adsorption measurements.

Supplementary Material Available:

Partial charges of the zeolite framework atoms used in Monte Carlo calculations, XRD diffraction pattern for the bulk $Ce(NO_3)_3.4H_2O$, FAU zeolite structure showing the principal crystallographic sites for the location of charge-compensating cations, snapshots of the unit cell for experimental and model zeolite structures at different temperatures and hydration states, TGA mass loss and heat release profiles of the zeolite samples studied.

REFERENCES

[1] L. Pérez-Lombard, J. Ortiz, C. Pout, A review on buildings energy consumption information, Energy Build. 40 (2008) 394–398. doi:10.1016/j.enbuild.2007.03.007.

[2] P. Tatsidjodoung, N. Le Pierrès, L. Luo, A review of potential materials for thermal energy storage in building applications, Renew. Sustain. Energy Rev. 18 (2013) 327–349. doi:10.1016/j.rser.2012.10.025.

[3] N. Yu, R.Z. Wang, L.W. Wang, Sorption thermal storage for solar energy, Prog. Energy Combust. Sci. 39 (2013) 489–514. doi:10.1016/j.pecs.2013.05.004.

[4] K.E. N'Tsoukpoe, H. Liu, N. Le Pierrès, L. Luo, A review on long-term sorption solar energy storage, Renew. Sustain. Energy Rev. 13 (2009) 2385–2396. doi:10.1016/j.rser.2009.05.008.

[5] S. Kiyabu, J.S. Lowe, A. Ahmed, D.J. Siegel, Computational screening of hydration reactions for thermal energy storage: new materials and design rules, Chem. Mater. 30 (2018) 2006–2017. doi:10.1021/acs.chemmater.7b05230.

[6] H. Wu, F. Salles, J. Zajac, A critical review of solid materials for low-temperature thermochemical storage of solar energy based on solid-vapour adsorption in view of space heating uses, Molecules. 24 (2019) 945. doi:10.3390/molecules24050945.

[7] C. Bales, P. Gantenbein, A. Hauer, H.-M. Henning, D. Jaenig, H. Kerskes, et al., Report B2 of subtask B: Thermal properties of materials for thermo-chemical storage of solar heat : a technical report of Subtask B, 2005. Consulted on 11th September 2018.

[8] L. Navarro, A. de Gracia, S. Colclough, M. Browne, S.J. McCormack, P. Griffiths, et al., Thermal energy storage in building integrated thermal systems: A review. Part 1. active storage systems, Renew. Energy. 88 (2015) 526–547. doi:10.1016/j.renene.2015.11.040.

[9] H. Deshmukh, M.P. Maiya, S. Srinivasa Murthy, Study of sorption based energy storage system with silica gel for heating application, Appl. Therm. Eng. 111 (2017) 1640–1646. doi:10.1016/j.applthermaleng.2016.07.069.

[10] S. Mitra, N. Aswin, P. Dutta, Scaling analysis and numerical studies on water vapour adsorption in a columnar porous silica gel bed, Int. J. Heat Mass Transf. 95 (2016) 853–864. doi:10.1016/j.ijheatmasstransfer.2015.12.011.

[11] A. Jabbari-Hichri, S. Bennici, A. Auroux, Effect of aluminum sulfate addition on the thermal storage performance of mesoporous SBA-15 and MCM-41 materials, Sol. Energy Mater. Sol. Cells. 149 (2016) 232–241. doi:10.1016/j.solmat.2016.01.033.

[12] A. Khutia, H.U. Rammelberg, T. Schmidt, S. Henninger, C. Janiak, Water sorption cycle measurements on functionalized MIL-101Cr for heat transformation application, Chem. Mater. 25 (2013) 790–798. doi:10.1021/cm304055k.

[13] J. Canivet, A. Fateeva, Y. Guo, B. Coasne, D. Farrusseng, Water adsorption in MOFs: fundamentals and applications., Chem. Soc. Rev. (2014) 5594–5617. doi:10.1039/c4cs00078a.

[14] M.F. De Lange, K.J.F.M. Verouden, T.J.H. Vlugt, J. Gascon, F. Kapteijn, Adsorption-

driven heat pumps: the potential of metal-organic frameworks, Chem. Rev. 115 (2015) 12205–12250. doi:10.1021/acs.chemrev.5b00059.

[15] S.K. Henninger, H.A. Habib, C. Janiak, MOFs as adsorbents for low temperature heating and cooling applications, J. Am. Chem. Soc. 131 (2009) 2776–2777. doi:10.1021/ja808444z.

[16] B. Mette, H. Kerskes, H. Drück, H. Müller-Steinhagen, Experimental and numerical investigations on the water vapor adsorption isotherms and kinetics of binderless zeolite 13X, Int. J. Heat Mass Transf. 71 (2014) 555–561. doi:10.1016/j.ijheatmasstransfer.2013.12.061.

[17] D. Lefebvre, F.H. Tezel, A review of energy storage technologies with a focus on adsorption thermal energy storage processes for heating applications, Renew. Sustain. Energy Rev. 67 (2017) 116–125. doi:10.1016/j.rser.2016.08.019.

[18] R.A. Shigeishi, C.H. Langford, B.R. Hollebone, Solar energy storage using chemical potential changes associated with drying of zeolites, Sol. Energy. 23 (1979) 489–495. doi:http://dx.doi.org/10.1016/0038-092X(79)90072-0.

[19] T. Schmidt, D. Mangold, H. Müller-Steinhagen, Central solar heating plants with seasonal storage in Germany, Sol. Energy. 76 (2004) 165–174. doi:https://doi.org/10.1016/j.solener.2003.07.025.

[20] G. Storch, G. Reichenauer, F. Scheffler, A. Hauer, Hydrothermal stability of pelletized zeolite 13X for energy storage applications, Adsorption. 14 (2008) 275–281. doi:10.1007/s10450-007-9092-7.

[21] K.M. Kim, H.T. Oh, S.J. Lim, K. Ho, Y. Park, C.H. Lee, Adsorption equilibria of water vapor on zeolite 3A, zeolite 13X, and dealuminated Y zeolite, J. Chem. Eng. Data. 61 (2016) 1547–1554. doi:10.1021/acs.jced.5b00927.

[22] J.C. Moïse, J.P. Bellat, A. Méthivier, Adsorption of water vapor on X and Y zeolites exchanged with barium, Microporous Mesoporous Mater. 43 (2001) 91–101. doi:10.1016/S1387-1811(00)00352-8.

[23] P. Aprea, B. de Gennaro, N. Gargiulo, A. Peluso, B. Liguori, F. Iucolano, et al., Sr-, Zn- and Cd-exchanged zeolitic materials as water vapor adsorbents for thermal energy storage applications, Appl. Therm. Eng. 106 (2016) 1217–1224.

doi:10.1016/j.applthermaleng.2016.06.066.

[24] F. Salles, J.M. Douillard, O. Bildstein, C. Gaudin, B. Prelot, J. Zajac, et al., Driving force for the hydration of the swelling clays: Case of montmorillonites saturated with alkaline-earth cations, J. Colloid Interface Sci. 395 (2013) 269–276. doi:10.1016/j.jcis.2012.12.050.

[25] F. Salles, J.-M. Douillard, O. Bildstein, S. El Ghazi, B. Prélot, J. Zajac, et al., Diffusion of interlayer cations in swelling clays as a function of water content: case of montmorillonites saturated with alkali cations, J. Phys. Chem. C. 119 (2015) 10370–10378. doi:https://doi.org/10.1021/jp512986d.

[26] D. Alby, F. Salles, J. Fullenwarth, J. Zajac, On the use of metal cation-exchanged zeolites in sorption thermochemical storage: Some practical aspects in reference to the mechanism of water vapor adsorption, Sol. Energy Mater. Sol. Cells. 179 (2018) 223–230. doi:https://doi.org/10.1016/j.solmat.2017.11.020.

[27] A. Di Lella, N. Desbiens, A. Boutin, I. Demachy, P. Ungerer, J.-P. Bellat, et al., Molecular simulation studies of water physisorption in zeolites., Phys. Chem. Chem. Phys. 8 (2006) 5396–406. doi:10.1039/b610621h.

[28] C. Abrioux, B. Coasne, G. Maurin, F. Henn, M. Jeffroy, A. Boutin, Cation behavior in faujasite zeolites upon water adsorption: A combination of Monte Carlo and molecular dynamics simulations, J. Phys. Chem. C. 113 (2009) 10696–10705. doi:10.1021/jp902274t.

[29] Y. Marcus, A simple empirical model describing the thermodynamics of hydration of ions of widely varying charges, sizes, and shapes, Biophys. Chem. 51 (1994) 111–127. doi:10.1016/0301-4622(94)00051-4.

[30] D.W. Smith, Ionic hydration enthalpies, J. Chem. Educ. 54 (1977) 540. doi:10.1021/ed054p540.

[31] J. Paier, C. Penschke, J. Sauer, Oxygen defects and surface chemistry of Ceria: quantum cemical studies compared to experiment, Chem. Rev. 113 (2013) 3949–3985. doi:doi.org/10.1021/cr3004949.

[32] F.D. Hunter, Cation positions in Cerium X zeolites, J. Catal. 246259 (1971) 246–259. doi:doi.org/10.1016/0021-9517(71)90086-8.

[33] F. Rouquerol, L. Luciani, P. Llewellyn, R. Denoyel, J. Rouquerol, Texture des matériaux pulvérulents ou poreux, Tech. l'Ingénieur. P1050 (2003) 1–24.

[34] L. Palatinus, Superflip — A computer program for solution of crystal structures from X-ray diffraction data in arbitrary dimension. User manual, Lausanne, 2007.

[35] V. Petrícek, M. Dušek, L. Palatinus, Crystallographic computing system JANA2006: General features, Zeitschrift Fur Krist. 229 (2014) 345–352. doi:10.1515/zkri-2014-1737.

[36] N. Tanchoux, P. Trens, D. Maldonado, F. Di Renzo, F. Fajula, The adsorption of hexane over MCM-41 type materials, Colloids Surfaces A Physicochem. Eng. Asp. 246 (2004) 1–8. doi:10.1016/j.colsurfa.2004.06.033.

[37] P. Trens, H. Belarbi, C. Shepherd, P. Gonzalez, N.A. Ramsahye, U.H. Lee, et al., Coadsorption of n -hexane and benzene vapors onto the chromium terephthalate-based porous material MIL-101(Cr) an experimental and computational study, J. Phys. Chem. C. 116 (2012) 25824–25831. doi:10.1021/jp308258k.

[38] J. Zajac, R. Dutartre, D.J. Jones, J. Roziere, Determination of surface acidity of powdered porous materials based on ammonia chemisorption: comparison of flow-microcalorimetry with batch volumetric method and temperature- programmed desorption, Thermochim. Acta. 379 (2001) 123–130. doi:10.1016/S0040-6031(01)00611-6.

[39] G. Vitale, C.F. Mellot, L.M. Bull, A.K. Cheetham, Neutron diffraction and computational study of zeolite NaX: influence of SIII' cations on its complex with benzene, J. Phys. Chem. B. 101 (1997) 4559–4564. doi:10.1021/jp970393x.

[40] A. Sartbaeva, S.A. Wells, M.M.J. Treacy, M.F. Thorpe, The flexibility window in zeolites, Nat. Mater. 5 (2006) 962–965. doi:10.1038/nmat1784.

[41] Ş.Ç. Sayilgan, M. Mobedi, S. Ülkü, Effect of regeneration temperature on adsorption equilibria and mass diffusivity of zeolite 13X-water pair, Microporous Mesoporous Mater. 224 (2016) 9–16. doi:10.1016/j.micromeso.2015.10.041.

[42] J. Hunger, I.A. Beta, H. Böhlig, C. Ling, H. Jobic, B. Hunger, Adsorption structures of water in NaX studied by DRIFT spectroscopy and neutron powder diffraction, J. Phys. Chem. B. 110 (2006) 342–353. doi:10.1021/jp054636u.

[43] D. H.Olson, The crystal-structure of dehydrated NaX, Zeolites. 15 (1995) 439–443. doi:https://doi.org/10.1016/0144-2449(95)00029-6.

[44] C. Abrioux, B. Coasne, G. Maurin, F. Henn, A. Boutin, A. Di Lella, et al., A molecular simulation study of the distribution of cation in zeolites, Adsorption. 14 (2008) 743–754. doi:10.1007/s10450-008-9123-z.

[45] M. Jeffroy, A. Boutin, A.H. Fuchs, Understanding the equilibrium ion exchange properties in faujasite zeolite from Monte Carlo simulations, J. Phys. Chem. B. 115 (2011) 15059–15066. doi:10.1021/jp209067n.

[46] M. Jeffroy, E. Borissenko, A. Boutin, A. Di Lella, F. Porcher, M. Souhassou, et al., Evidence of a framework induced cation redistribution upon water adsorption in cobalt exchanged X faujasite zeolite: A joint experimental and simulation study, Microporous Mesoporous Mater. 138 (2011) 45–50. doi:10.1016/j.micromeso.2010.09.031.

[47] M. Jeffroy, C.N. Draghi, A. Boutin, A new molecular simulation method to determine both aluminum and cation location in cationic zeolites, Chem. Mater. 29 (2017) 513–523. doi:10.1021/acs.chemmater.6b03011.